TGF-β blockade controls ascites by preventing abnormalization of lymphatic vessels in orthotopic human ovarian carcinoma models

Shan Liao[1], **Jieqiong Liu**[1,2], **Peichun Lin**[1], **Tony Shi**[3], **Rakesh K. Jain**[1], and **Lei Xu**[1]

[1]Edwin L. Steele Laboratory, Department of Radiation Oncology, Massachusetts General Hospital, Boston, Massachusetts 02114

[2]Department of Breast Surgery, the Second Xiangya Hospital of Central South University, Changsha, Hunan, China 410001

[3]College of Arts and Sciences, New York University, New York, NY 10012

Abstract

Purpose—Ovarian cancer patients with malignant ascites have poor prognosis. The accumulation of ascites is caused by an imbalance between fluid extravasation from the blood vessels and reabsorption by lymphatic vessels. Whereas, the role of Transforming Growth Factor beta (TGF-β) in tumor progression has been well studied, the role of TGF-β in lymphatic vessel function is far from understood. Here, we sought to dissect the role of TGF-β blockade in the formation of ascites.

Experimental Design—We used soluble TGF-β Receptor II (sTβRII) to block TGF-β signaling in two orthotopic human ovarian carcinoma models: SKOV3ip1 and Hey-A8. We measured tumor proliferation, apoptosis, lymphangiogenesis and angiogenesis by immunohistochemical staining, and examined diaphragm lymphatic vessel network by intraperitoneal injection of a fluorescent dye. Diaphragm lymphatic vessel function was assessed by tracking fluorescent beads in the diaphragm and measuring their drainage rate.

Results—TGF-β blockade impaired tumor growth in both models, accompanied by a decreased tumor cell proliferation and angiogenesis. More strikingly, TGF-β blockade almost completely abolished ascites formation. TGF-β blockade significantly inhibited the expression of VEGF, which is the major contributor to ascites formation. At the same time, TGF-β blockade prevent 'abnormalization' of diaphragm lymphatic vessels and improved ascites drainage.

Conclusions—TGF-β blockade decreased ascites by both inhibiting ascites formation and improving ascites drainage. Based on our finding, it is reasonable to consider the use of TGF-β blockade as a palliative treatment for symptomatic ascites.

Introduction

Ovarian cancer is characterized by rapid growth of peritoneal tumors and accumulation of ascites (1). When present in large amounts, ascites increases abdominal pressure and leads to pain, loss of appetite, nausea and reduced mobility. In addition to tumor eradication, symptomatic relief from ascites becomes a primary therapeutic goal for many patients. Therapeutic options are limited to paracentesis and diuretics followed by peritoneovenous shunts, diet measures and other modalities like systemic or intraperitoneal chemotherapy (2).

[1]Correspondence to: Lei Xu, MD, Ph.D., lei@steele.mgh.harvard.edu.

However, these treatments only temporarily alleviate the symptoms and can induce adverse effects and discomfort. In contrast to the treatment of underlying cancer, so far there is no generally accepted evidence-based guideline for the management of malignant ascites.

The ascites results from excessive production and impaired drainage of intraperitoneal fluid (3,4). Vascular Endothelial Growth Factor/Vascular Permeability Factor (VEGF/VPF) is crucial for the production of malignant ascites (3). Avastin, a recombinant humanized monoclonal antibody to VEGF, has been shown to reduce ascites (5). However, it only inhibits the production of peritoneal fluid but does not affect ascites drainage. Lymphatic vessels in the diaphragm drain peritoneal fluid (6). We have previously shown that lymphatic vessels in hyperplastic, dysplastic and neoplastic lesions are compressed and nonfunctional (7). Indeed, relieving the compressive mechanical stress opens up lymphatic vessels, however, these vessels still remain non-functional, presumably due to irreversible damage in the lymphatic valves (8,9). We and others have been shown both pre-clinically and clinically that anti-angiogenic therapy can "normalize" tumor blood vessels (10–12). However, there are no studies on how to normalize lymphatic vessels. Here, we show that TGF-β blockade inhibits ascites production (via inhibition of VEGF production) and prevents 'abnormalization' of lymphatic vessel function, resulting in almost complete control of malignant ascites. Our findings suggest TGF-β blockade should be explored as a palliative option in end-stage ovarian carcinoma patients with symptomatic ascites.

Methods

Cell lines

SKOV3 ip1 and Hey-A8 cells were gifts from Dr. Isaiah J. Fidler (M.D. Anderson Cancer Center, Houston, TX). Mv1Lu cells were obtained from ATCC (Manassas, VA).

Plasmid construction

Mouse TGF-β receptor II extracellular domain was amplified from a mouse heart cDNA library and cloned into peak13CD5 vector, which contains a CD5 leader upstream of the human IgG1 hinge region sequences (a gift from Dr. Brian Seed, Center for Computational and Integrative Biology, Massachusetts General Hospital).

Purification and activity of the sTβRII

The sTβRII constructs were transfected into 293 cells by Lipofectamine 2000 (Invitrogen, Calsbad, CA). Following overnight incubation, cells were washed with PBS and changed to fresh medium containing 0% FBS. After 3 days of incubation, the supernatant was collected and centrifuged; recombinant sTβRII was purified with Protein A Sepharose chromatography in accordance with manufacturer's protocol (Chemicon International, Temecula, CA). To determine the activity of sTβRII, serial dilutions of sTβRII was incubated for 1hr with 0.1 ng/ml TGF-β1, 0.5 ng/ml TGF-β2 and 0.05 µg/ml TGF-β3 (R&D Systems, Minneapolis, MN), and then added to Mv1Lu cells (13). Cell proliferation was determined by [^{3}H]TdR incorporation assay (14).

Orthotopic implantation

SKOV3ip1 and Hey-A8 tumor cells were injected *i.p.* into female nude mice (1×10^6 cells/ mice). Intraperitoneal injection of tumor cells produced solid tumors grown on the surface of the peritoneal organs and tumors invaded into the diaphragm. Mice bearing SKOV3ip1 tumors also produced large amount of ascites. Mice were sacrificed 35 days later. Peritoneal tumors were excised and weighed. Malignant ascites were aspirated and measured (14).

Northern blot analysis

Northern blot was performed as described previously (15). cDNA probes were synthesized by PCR, using the following primers: IL-8F: 5'-CGG ACA GAC AGA CAG ACA CC-3'; IL-8R: 5'-AAG AAA ACT GGG TGC AGA G-3'. VEGF-F: 5'-AAG GAG GAG GGC AGA ATC AT-3'; VEGF-R: 5'-AAA AAC GAA AGC GCA AGA AA-3'.

ELISA

Tumor tissue was lysed to extract protein, and IL-8 and VEGF were quantified using Quantikine ELISA kit (R&D Systems, Minneapolis, MN). IL-8 and VEGF levels (pg/ml) were normalized by the amount of total protein measured using Dc Protein Assay (Bio-Rad, Hercules, CA) (mg/ml) (16).

Western blot analysis

Cells or tumor tissue was lysed to extract protein (16). 30 µg of protein per sample was separated on SDS-polyacrylamide gels (17). Phosphorylation status of SMAD was detected by phosphor-specific antibodies (Manufacturer, City, State).

Immunohistochemistry

Tissue sections (5 µm thick) of formalin-fixed, paraffin-embedded tumor xenografts were deparaffinized in xylene and rehydrated in graded alcohol. The endogenous peroxidase was blocked with the addition of 3% hydrogen peroxide in PBS for 12 min. The samples were incubated for 20 min at room temperature with protein-blocking solution [PBS (pH 7.5) containing 5% normal horse serum and 1% normal goat serum] followed by incubation at 4°C with primary antibodies (anti-CD31, 1:800, BD Biosciences, Franklin Lake, NJ; anti-Proliferating Cell Nuclear Antigen (PCNA), 1:50, Dako Corporation, Capinteria, CA; F4/80, 1:10, Serotec, Raleigh, NC; LYVE-1 and α-SMA). The samples were then rinsed and incubated for 1 hour at room temperature with a peroxidase-conjugated anti-rabbit IgG. The slides were rinsed with PBS and incubated for 5 min with diaminobenzidine. The sections were then washed three times with distilled water, counterstained with Mayer's hematoxylin, washed once with distilled water and once more with PBS. The slides were mounted with a universal mount and examined with a bright-field microscope (18).

TUNEL

For TUNEL staining, tissue samples were fixed in 4% (w/v) paraformaldehyde in phosphate-buffered saline. Paraffin-embedded sections (5 µm) were used for *in situ* detection of apoptotic cells. After deparaffinization and rehydration, tissue sections were stained with terminal deoxynucleotidyl transferase and incubated with diaminobenzidine. The sections were counterstained with Methyl Green, and the percentage of TUNEL-positive cells was quantified (Millipore, Billerica, MA)(19).

Functional assays for lymphatic vessel drainage

Four weeks after cell implantation, mice were injected *i.p.* with fluorescent beads (0.2 ml, 1 µm in diameter). Two hours later, diaphragms were harvested and fixed with 4% paraformaldehyde for fluorescent microscopy. Claudal mediastinal lymph node (CMLNs) were harvested and homogenized to measure fluorescence intensity with fluorescent plate reader (Perkin Elmer, Boston, MA).

Diphtheria toxin treatment

When SKOV3ip1 tumor bearing mice developed visible ascites, diphtheria toxin (1 mg) or PBS was injected *i.p.* (8). 5 days later, mice were sacrificed to test lymphatic function.

Data analysis and interpretation

All data are presented as mean ± SD. The significance of differences between two groups was analyzed using the Student's *t* test (two tailed) or Mann-Whitney *U* test (two tailed).

Result

Characterization of sTβRII

We used two methods to block tumor and host TGF-β signaling. First we stably transfected the sTβRII construct into SKOV3ip1 and Hey-A8 cells. These transfected cells constitutively secreted large quantities of sTβRII protein (Fig. 1A, 1B). Second, we used purified recombinant sTβRII protein as a therapeutic agent. To test the function of the purified sTβRII protein, we treated Mv1Lu cells with recombinant TGF-β1, -β2 and -β3 in the presence or absence of purified sTβRII. Our purified sTβRII successfully blocked TGF-β1 and -β3 but not TGF-β2-mediated inhibition of cell proliferation (data not shown). It also blocked TGF-β1 induced phosphorylation of Smad2 (Fig. 1C).

Blocking tumor and host TGF-β signaling inhibits ovarian cancer growth and ascites formation

In the first group, we orthotopically implanted parental, mock- and sTβRII-transfected SKOV3ip1 (SKOV-sTβRII) and Hey-A8 (Hey-sTβRII) cells *i.p.* into nude mice. We examined peritoneal tumor weight at day 35. Transfection of sTβRII decreased tumor weight in both models (P<0.01). Mice implanted with SKOV3ip1 and mock-transfected cells formed large amounts of bloody ascites, whereas transfection of sTβRII almost completely abolished ascites formation (Fig. 2A–B).

In the second group, we implanted parental SKOV3ip1 and Hey-A8 cells *i.p.* into nude mice. 7 days after tumor implantation, we began treatment with control IgG or recombinant sTβRII protein (1 mg/kg, *i.p.*, every three days). Recombinant sTβRII treatment significantly inhibited tumor growth (P<0.01). More dramatically, sTβRII treatment almost completely abolished ascites formation (Fig. 2C–D, P<0.001).

Blocking tumor and host TGF-β signaling inhibits tumor cell proliferation and angiogenesis via inhibition of IL-8 and VEGF expression

VEGF and Interleukin 8 (IL-8) are angiogenic and autocrine growth factors for ovarian tumors (20). In TGF-β blocked tumors, VEGF and IL-8 mRNA and protein decreased significantly (Fig. 3A–B). As a result, we found the number of PCNA^{+} cells decreased significantly in TGF-β blocked tumors (SKOV3-sTβRII: 36 ± 13; Hey-sTβRII: 62 ± 27) compared to parental tumors (SKOV3ip1: 128 ± 25; Hey-A8: 142 ± 22; data shown as number of PCNA^{+} cells per 0.329 mm^2 area) (P<0.001). We also found parental tumors had significantly more CD31^{+} endothelial cells (SKOV3ip1: 62 ± 7; Hey-A8: 48 ± 4) than sTβRII tumors (SKOV3-sTβRII: 22 ± 4; Hey-sTβRII: 16 ± 6, Fig. 3C) (P<0.001, data are shown as number of CD31^{+} structures per 1.355 mm^2).

Tumor associated macrophages (TAMs) play an important role in tumor progression (6). We examined the effect of TGF-β blockade on TAM infiltration in peritoneal ovarian tumors using the macrophage marker F4/80. A lower infiltrating macrophage density was detected in SKOV-sTβRII tumors (52 ± 16) than in SKOV3ip1 tumors (145 ± 22, P<0.001, data are shown as number of F4/80^{+} cells per 1.335 mm^2).

Blocking tumor and host TGF-β signaling prevented abnormalization of diaphragm lymphatic vessel network

We examined the diaphragm lymphatics by fluorescence lymphangiography (FITC-dextran, 0.2 ml, 2×10^6 MW, i.p.). Twenty minutes later, diaphragms were collected and observed under fluorescence microscopy. In non-tumor bearing mice, we observed the distinct outline of organized lymphatic strips on the peritoneal side of the diaphragm. In mice bearing SKOV3ip1 tumors, the diaphragms contained lymphatic vessels of increased density and branching. In SKOV-sTβRII tumor-bearing mice, lymphatic strips appeared similar to those in normal mice. On the pleural side of the diaphragms, the dye showed normal lymphatic network in non-tumor bearing mice, an enlarged arrangement of lymphatic vessels in mice bearing SKOV3ip1 tumors and a 'normalized' lymphatic network in mice with SKOV-sTβRII tumors (Fig. 4A). Quantification data showed TGF-β blockade decreased diameter of lymphatic vessels on the pleural side (Fig. 4B).

Normal lymphatic vessels have one-way valves to prevent fluid from flowing backwards (21). We visualized lymphatic valves using CD31 and LYVE-1 double staining in whole mounts of the diaphragm. In parental tumors, profound lymphangiogenesis occurred and lymphatic valve structures disappeared completely – similar to our previous observations (9). In contrast, in TGF-β blocked tumors, normal lymphatic network was present and valve structures remained intact (Fig. 4C).

Blocking tumor and host TGF-β signaling decreased diaphragm lymphangiogenesis

In peritoneal tumors attached to the surface of peritoneal organs, we found little LYVE-1 immunostaining (data not shown). However, in tumors invading the diaphragms, LYVE-1 immunostaining showed that lymphatic vessels were abundant, enlarged and irregularly shaped. In diaphragms with invading SKOV-sTβRII tumors, lymphatic vessel density (in size-matched tumors in the diaphragm) had decreased (Fig. 5).

We further analyzed the number of infiltrating macrophages in (size-matched) tumors invading the diaphragm. In diaphragms from non-tumor bearing mice, using staining with CD11b (an alternative marker for macrophages), we found no infiltrating macrophages. In mice with SKOV3ip1 tumors, we identified a high number of macrophages (these cells being closely associated with LYVE-1 positive lymphatic vessels) (Fig. 5). In diaphragms with invading SKOV-sTβRII tumor, we identified the same amount of positive CD11b staining, but a reduced number of LYVE-1 positive vessels. This observation indicates that despite the presence of a large number of macrophage, these cells still require the presence of TGF-β to induce lymphangiogenesis.

Blocking tumor and host TGF-β signaling improved lymphatic vessel function

To study whether TGF-β blockade affects the function of diaphragm lymphatic vessels, we injected fluorescent beads intraperitoneally. In non-tumor bearing mice, few beads were observed in the diaphragm two hours after injection, indicating their clearance through the lymphatic vessels. In SKOV3ip1 tumor-bearing mice, despite the large number of lymphatic vessels, many beads remained in the diaphragm, indicating impaired drainage. In SKOV-sTβRII tumor-bearing mice, few beads were present (Fig. 6A).

Diaphragm lymphatic vessels drain into the claudal mediastinal lymph node (CMLN). To confirm and quantify drainage, we measured fluorescence intensity of beads drained to CMLN. Compared to mice with normal drainage, CMLNs from SKOV3ip1 tumor bearing mice had low fluorescence intensity, indicating decreased drainage. CMLNs from SKOV-sTβRII tumor bearing mice showed high fluorescence intensity (Fig. 6B), indicating TGF-β blockade improved drainage to CMLN.

This functional normalization may be attributed to TGF-β decreasing tumor weight, thus relieving the compression of lymphatic vessels (8). Indeed, we observed that in mice treated with diphtheria toxin (DT), which is much less cytotoxic to mouse than to human cells, ascites were resolved to a similar extent as in sTβRII treated mice (Control group: 3.5 ± 1.7 ml, DT group: 0.1 ± 0.3 ml).

Discussion

TGF-β is a multifunctional cytokine. Depending on the context, it can act on the tumor cells to increase epithelial to mesenchymal transition (EMT), migration, invasion and survival. It can act on stromal cells to induce angiogenesis and dampen local immune surveillance (22–24). Recent studies also showed TGF-β to affect intratumoral distribution of chemotherapeutic agents (25,26). We chose to study TGF-β because both TGF-β and its receptors are overexpressed in ovarian carcinomas, and because genes in the TGF-β signaling pathway are dysregulated in ovarian carcinomas (27). Several strategies to block TGF-β are being tested in various stages of investigation, from the laboratory to phase III clinical trials (28). These strategies fall into two categories: direct inhibition of TGF-β (via TGF-β neutralizing antibodies, soluble TGF-β receptors and decorin) and interference with the downstream signaling cascades (e.g., interferon-γ, peroxisome proliferator activated receptor-γ agonist). Soluble TGF-β receptor II competes with cell-bound TβRII for active TGF-β ligand, resulting in reduced TGF-β signaling. We chose to use this strategy because it has been shown that TGF-β1 and -β3 play a greater role in ovarian cancer progression than TGF-β2 (29), and sTβRII has been shown to specifically block the effects of TGF-β1 and -β3 (26).

In our study, we utilized a well-established human ovarian carcinoma orthotopic model in nude mice. When human ovarian cancer cells were injected orthotopically (intraperitoneal) into nude mice, they produced solid tumors that invaded the surface of peritoneal organs and diaphragm, and these tumors formed ascites. This growth pattern mimics the growth of human ovarian cancer in patients. We used two methods to block tumor and host TGF-β signaling. First, we established sTβRII-over-producing ovarian tumor cells (genetic approach). Second, we treated tumor-bearing mice with recombinant sTβRII (pharmacologic approach). A previous study showed that five days after tumor cell *i.p.* injection, diaphragmatic lymph vessels become occluded (30,31). In our study, we also observed small tumors established on the diaphragm and in the peritoneal cavity 7 days after tumor implantation. This tumor burden mimics that in patients after cytoreductive surgery and adjuvant chemotherapy. Based on these published studies and our own observations, we started sTβRII treatment 7 days after tumor implantation, when tumor lesions and obstruction of lymphatics were established.

Targeted therapy often fails because different tumors depend on different growth/angiogenic factors for their progression. The outcome of a therapy using specific inhibitors depends on the expression level of the target in the tumor, which varies significantly between patients. In addition, malignant tumors often switch growth factor dependence, thus permitting 'therapeutic escape' from specific, targeted drugs (15). In our study, we used two human ovarian carcinoma cell lines to represent cancer heterogeneity. SKOV3ip1 cells express high levels of VEGF and low levels of IL-8. When implanted orthotopically into the peritoneal cavity of nude mice, these cells formed solid tumors with large volumes of ascites. On the other hand, Hey-A8 cells express high levels of IL-8 and low levels of VEGF; when implanted into the peritoneal cavity, they formed solid tumors with little ascites (32). Previous study using PTK787, a VEGFR2 tyrosine kinase inhibitor, to block VEGF pathways has shown that inhibition of VEGF was only effective in inhibiting the growth of VEGF-dependent SKOV3ip1 tumors but not IL-8 dependent Hey-A8 tumors (14). TGF-β

stands at the crossroad of diverse signaling pathways, therefore, targeting TGF-β would have the advantage of bypassing the two problems – pointed out above - associated with VEGF- or IL8-targeted therapies. Indeed, in our study, we observed TGF-β blockade inhibited the expression of both VEGF and IL-8. As a result, TGF-β blockade effectively inhibited the progression of both VEGF-dependent (SKOV3ip1) and IL8-dependent (Hey-A8) human ovarian tumor xenografts.

The pathogenesis of malignant ascites is well elucidated. Increased fluid production and decreased lymphatic absorption are identified as contributing factors of ascites formation. In our study, we administered sTβRII intraperitoneally and showed a dual effect on ascites production and drainage. Tumors exhibit extensive angiogenesis, but tumor blood vessels are structurally and functionally abnormal (11). These vascular abnormalities contribute to high vessel permeability. Decreasing permeability of tumor vessels by inhibiting VEGF signaling using VEGF trap (soluble decoy receptor) or a VEGF neutralizing antibody has been shown to inhibit the formation of malignant ascites (33–35). TGF-β blockade has been shown to recruit pericyte and induce blood vessel 'normalization' (26); this, combined with our data showing TGF-β blockade inhibits VEGF production, provides a mechanism for decreased ascites production.

Furthermore, we studied the effect of TGF-β blockade on ascites drainage by examining vessel morphology and function of diaphragm lymphatics. The function of TGF-β on tumor growth and progression has been studied extensively (36), however, its effect on lymphangiogenesis was only recently studied (6,37,38). Therefore, its effect and underlying mechanisms on lymphatic vessel function remain largely unknown. Recent studies showed TGF-β can directly block lymphatic regeneration (in wound healing) and signal transduction in lymphatic endothelial cells (37,38). TGF-β can also increase the secretion of lymphangiogenic factors, thus indirectly enhancing lymphangiogenesis (6). The net result depends on the balance of the response to TGF-β. In our study, we observed that peritoneal ovarian tumors induced profound lymphangiogenesis in the diaphragm. However, these newly formed lymphatic vessels are not functional. Based on previous studies, which showed diaphragmatic lymph vessels becoming occluded five days after intraperitoneal injection of tumor cells (30,31), we administered *i.p.* sTβRII seven days after tumor implantation. We showed TGF-β blockade decreased lymphangiogenesis, reduced tumor burden in the diaphragm and maintained the normal lymphatic vessel morphology and valve structure. As a result, it improved the drainage function of diaphragm lymphatic vessels. This dual effect of TGF-β blockade on ascites production and drainage explains why it is a more efficient strategy than blocking VEGF alone (e.g., treatment with PTK787 leads to a 50% decrease in ascites volume, whereas sTβRII decreased ascites volume by 98%) (39).

In summary, our study shows that by blocking tumor and host TGF-β signaling we can significantly inhibit the growth of both VEGF- and IL-8-dependent human ovarian tumors. More importantly, we have shown that TGF-β blockade significantly decreases the volume of ascites by both inhibiting ascites formation and preventing impairment of lymphatic vessel drainage, thus demonstrating its potential as a new treatment for malignant ascites.

Translational Relevance

Ovarian cancer is characterized by the rapid growth of solid intraperitoneal tumors and accumulation of ascites, the ascites being the clinical presentation of end-stage disease. Whereas the role of Transforming Growth Factor beta (TGF-β) in tumor angiogenesis and progression is well understood, its role in lymphatic vessel function remains far from understood. To this end, we dissected the potential role of TGF-β blockade in controlling ascites using human ovarian cancer xenografts in mice. We found that blocking tumor

and host TGF-β signaling can significantly inhibit the growth of both VEGF- and IL-8-dependent human ovarian tumors. More importantly, we discovered that TGF-β blockade significantly decreases the volume of ascites by both inhibiting ascites formation and preventing impairment of lymphatic vessel drainage, thus demonstrating its potential as a promising new treatment for malignant ascites. Since a number of agents that target the TGF-β-pathway are in clinical trials, the results of the proposed study could be rapidly translated to the clinic.

Acknowledgments

Reference

1. Perez RP, Godwin AK, Hamilton TC, Ozols RF. Ovarian cancer biology. Semin Oncol. 1991; 18:186–204. [PubMed: 2042060]

2. Becker G, Galandi D, Blum HE. Malignant ascites: systematic review and guideline for treatment. Eur J Cancer. 2006; 42:589–597. [PubMed: 16434188]

3. Nagy JA, Masse EM, Herzberg KT, et al. Pathogenesis of ascites tumor growth: vascular permeability factor, vascular hyperpermeability, and ascites fluid accumulation. Cancer Res. 1995; 55:360–368. [PubMed: 7812969]

4. Intaglietta M, Zweifach BW. Microcirculatory basis of fluid exchange. Adv Biol Med Phys. 1974; 15:111–159. [PubMed: 4601204]

5. Numnum TM, Rocconi RP, Whitworth J, Barnes MN. The use of bevacizumab to palliate symptomatic ascites in patients with refractory ovarian carcinoma. Gynecol Oncol. 2006; 102:425–428. [PubMed: 16797681]

6. Kim KE, Koh YJ, Jeon BH, et al. Role of CD11b+ macrophages in intraperitoneal lipopolysaccharide-induced aberrant lymphangiogenesis and lymphatic function in the diaphragm. Am J Pathol. 2009; 175:1733–1745. [PubMed: 19762711]

7. Hagendoorn J, Tong R, Fukumura D, et al. Onset of abnormal blood and lymphatic vessel function and interstitial hypertension in early stages of carcinogenesis. Cancer Res. 2006; 66:3360–3364. [PubMed: 16585153]

8. Padera TP, Stoll BR, Tooredman JB, Capen D, di Tomaso E, Jain RK. Pathology: cancer cells compress intratumour vessels. Nature. 2004; 427:695. [PubMed: 14973470]

9. Isaka N, Padera TP, Hagendoorn J, Fukumura D, Jain RK. Peritumor lymphatics induced by vascular endothelial growth factor-C exhibit abnormal function. Cancer Res. 2004; 64:4400–4404. [PubMed: 15231646]

10. Jain RK. Normalizing tumor vasculature with anti-angiogenic therapy: a new paradigm for combination therapy. Nat Med. 2001; 7:987–989. [PubMed: 11533692]

11. Jain RK. Normalization of tumor vasculature: an emerging concept in antiangiogenic therapy. Science. 2005; 307:58–62. [PubMed: 15637262]

12. Gerstner ER, Duda DG, di Tomaso E, et al. VEGF inhibitors in the treatment of cerebral edema in patients with brain cancer. Nat Rev Clin Oncol. 2009; 6:229–236. [PubMed: 19333229]

13. Tsang ML, Zhou L, Zheng BL, et al. Characterization of recombinant soluble human transforming growth factor-beta receptor type II (rhTGF-beta sRII). Cytokine. 1995; 7:389–397. [PubMed: 7578976]

14. Xu L, Fidler IJ. Interleukin 8: an autocrine growth factor for human ovarian cancer. Oncol Res. 2000; 12:97–106. [PubMed: 11132928]

15. Izumi Y, Xu L, di Tomaso E, Fukumura D, Jain RK. Tumour biology: herceptin acts as an antiangiogenic cocktail. Nature. 2002; 416:279–280. [PubMed: 11907566]

16. Xu L, Cochran DM, Tong RT, et al. Placenta growth factor overexpression inhibits tumor growth, angiogenesis, and metastasis by depleting vascular endothelial growth factor homodimers in orthotopic mouse models. Cancer Res. 2006; 66:3971–3977. [PubMed: 16618713]

17. Xu L, Pathak PS, Fukumura D. Hypoxia-induced activation of p38 mitogen-activated protein kinase and phosphatidylinositol 3'-kinase signaling pathways contributes to expression of interleukin 8 in human ovarian carcinoma cells. Clin Cancer Res. 2004; 10:701–707. [PubMed: 14760093]

18. Xu L, Jain RK. Down-regulation of placenta growth factor by promoter hypermethylation in human lung and colon carcinoma. Mol Cancer Res. 2007; 5:873–880. [PubMed: 17704140]

19. Xu L, Tong R, Cochran DM, Jain RK. Blocking platelet-derived growth factor-D/platelet-derived growth factor receptor beta signaling inhibits human renal cell carcinoma progression in an orthotopic mouse model. Cancer Res. 2005; 65:5711–5799. [PubMed: 15994946]

20. Fidler IJ, Yoneda J, Herrera C, Wood J, Xu L. Specific keynote: molecular determinants of angiogenesis in ovarian cancer. Gynecol Oncol. 2003; 88:S29–S36. discussion S7-42. [PubMed: 12586082]

21. Schmid-Schonbein GW. The second valve system in lymphatics. Lymphat Res Biol. 2003; 1:25–29. [PubMed: 15624318]

22. Gorelik L, Flavell RA. Immune-mediated eradication of tumors through the blockade of transforming growth factor-beta signaling in T cells. Nat Med. 2001; 7:1118–1122. [PubMed: 11590434]

23. Gorelik L, Flavell RA. Transforming growth factor-beta in T-cell biology. Nat Rev Immunol. 2002; 2:46–53. [PubMed: 11905837]

24. Bierie B, Moses HL. Gain or loss of TGFbeta signaling in mammary carcinoma cells can promote metastasis. Cell Cycle. 2009; 8:3319–3327. [PubMed: 19806012]

25. Kano MR, Bae Y, Iwata C, et al. Improvement of cancer-targeting therapy, using nanocarriers for intractable solid tumors by inhibition of TGF-beta signaling. Proc Natl Acad Sci U S A. 2007; 104:3460–3465. [PubMed: 17307870]

26. Salnikov AV, Roswall P, Sundberg C, Gardner H, Heldin NE, Rubin K. Inhibition of TGF-beta modulates macrophages and vessel maturation in parallel to a lowering of interstitial fluid pressure in experimental carcinoma. Lab Invest. 2005; 85:512–521. [PubMed: 15711566]

27. Sunde JS, Donninger H, Wu K, et al. Expression profiling identifies altered expression of genes that contribute to the inhibition of transforming growth factor-beta signaling in ovarian cancer. Cancer Res. 2006; 66:8404–8412. [PubMed: 16951150]

28. Jakowlew SB. Transforming growth factor-beta in cancer and metastasis. Cancer Metastasis Rev. 2006; 25:435–457. [PubMed: 16951986]

29. Bristow RE, Baldwin RL, Yamada SD, Korc M, Karlan BY. Altered expression of transforming growth factor-beta ligands and receptors in primary and recurrent ovarian carcinoma. Cancer. 1999; 85:658–668. [PubMed: 10091739]

30. Fastaia J, Dumont AE. Pathogenesis of ascites in mice with peritoneal carcinomatosis. J Natl Cancer Inst. 1976; 56:547–550. [PubMed: 1255784]

31. Feldman GB, Knapp RC, Order SE, Hellman S. The role of lymphatic obstruction in the formation of ascites in a murine ovarian carcinoma. Cancer Res. 1972; 32:1663–1666. [PubMed: 5044130]

32. Yoneda J, Kuniyasu H, Crispens MA, Price JE, Bucana CD, Fidler IJ. Expression of angiogenesis-related genes and progression of human ovarian carcinomas in nude mice. J Natl Cancer Inst. 1998; 90:447–454. [PubMed: 9521169]

33. Hu L, Hofmann J, Holash J, Yancopoulos GD, Sood AK, Jaffe RB. Vascular endothelial growth factor trap combined with paclitaxel strikingly inhibits tumor and ascites, prolonging survival in a human ovarian cancer model. Clin Cancer Res. 2005; 11:6966–6971. [PubMed: 16203789]

34. Hu L, Hofmann J, Zaloudek C, Ferrara N, Hamilton T, Jaffe RB. Vascular endothelial growth factor immunoneutralization plus Paclitaxel markedly reduces tumor burden and ascites in athymic mouse model of ovarian cancer. Am J Pathol. 2002; 161:1917–1924. [PubMed: 12414537]

35. Byrne AT, Ross L, Holash J, et al. Vascular endothelial growth factor-trap decreases tumor burden, inhibits ascites, and causes dramatic vascular remodeling in an ovarian cancer model. Clin Cancer Res. 2003; 9:5721–5728. [PubMed: 14654557]

36. Moses HL, Yang EY, Pietenpol JA. TGF-beta stimulation and inhibition of cell proliferation: new mechanistic insights. Cell. 1990; 63:245–247. [PubMed: 2208284]

37. Oka M, Iwata C, Suzuki HI, et al. Inhibition of endogenous TGF-beta signaling enhances lymphangiogenesis. Blood. 2008; 111:4571–4579. [PubMed: 18310502]

38. Clavin NW, Avraham T, Fernandez J, et al. TGF-beta1 is a negative regulator of lymphatic regeneration during wound repair. Am J Physiol Heart Circ Physiol. 2008; 295:H2113–H2127. [PubMed: 18849330]

39. Xu L, Yoneda J, Herrera C, Wood J, Killion JJ, Fidler IJ. Inhibition of malignant ascites and growth of human ovarian carcinoma by oral administration of a potent inhibitor of the vascular endothelial growth factor receptor tyrosine kinases. Int J Oncol. 2000; 16:445–454. [PubMed: 10675474]
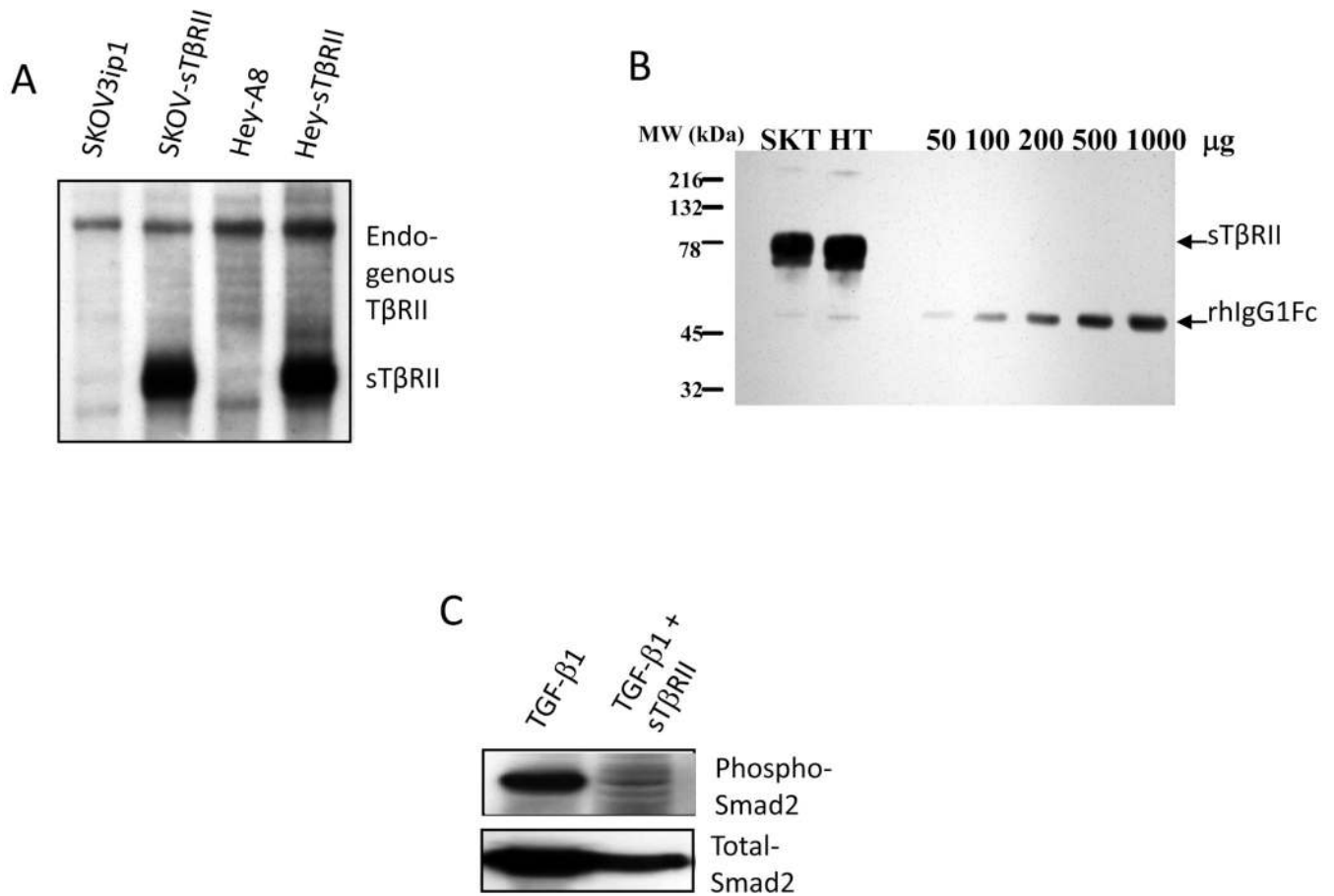
Figure 1.
Characterization of soluble TGF-β receptor type II. (A) Transfected cells overexpress sTβRII mRNA. Northern blot analysis of mRNA from parental SKOV3ip1, Hey-A8 cells and sTβRII transfected SKOV3ip1 (SKOV-STβRII) and Hey-A8 (Hey-STβRII) cells. (B) Transfected cells overexpress sTβRII protein. Supernatant collected from transfected SKOV3ip1 cells was subjected to 12% SDS-gel electrophoresis and Western blot analysis. Different amount of recombinant human IgG region was used as standard. (C) sTβRII blocks TGF-β induced Smad2 phosphorylation. SKOV3ip1 cells were treated with 10 ng/ml TGF-β1 alone or with TGF-β1 plus sTβRII (10μg/ml). Proteins were obtained and analyzed by western blot. The membrane was probed with antibody against phospho-Smad2 or total Smad2.
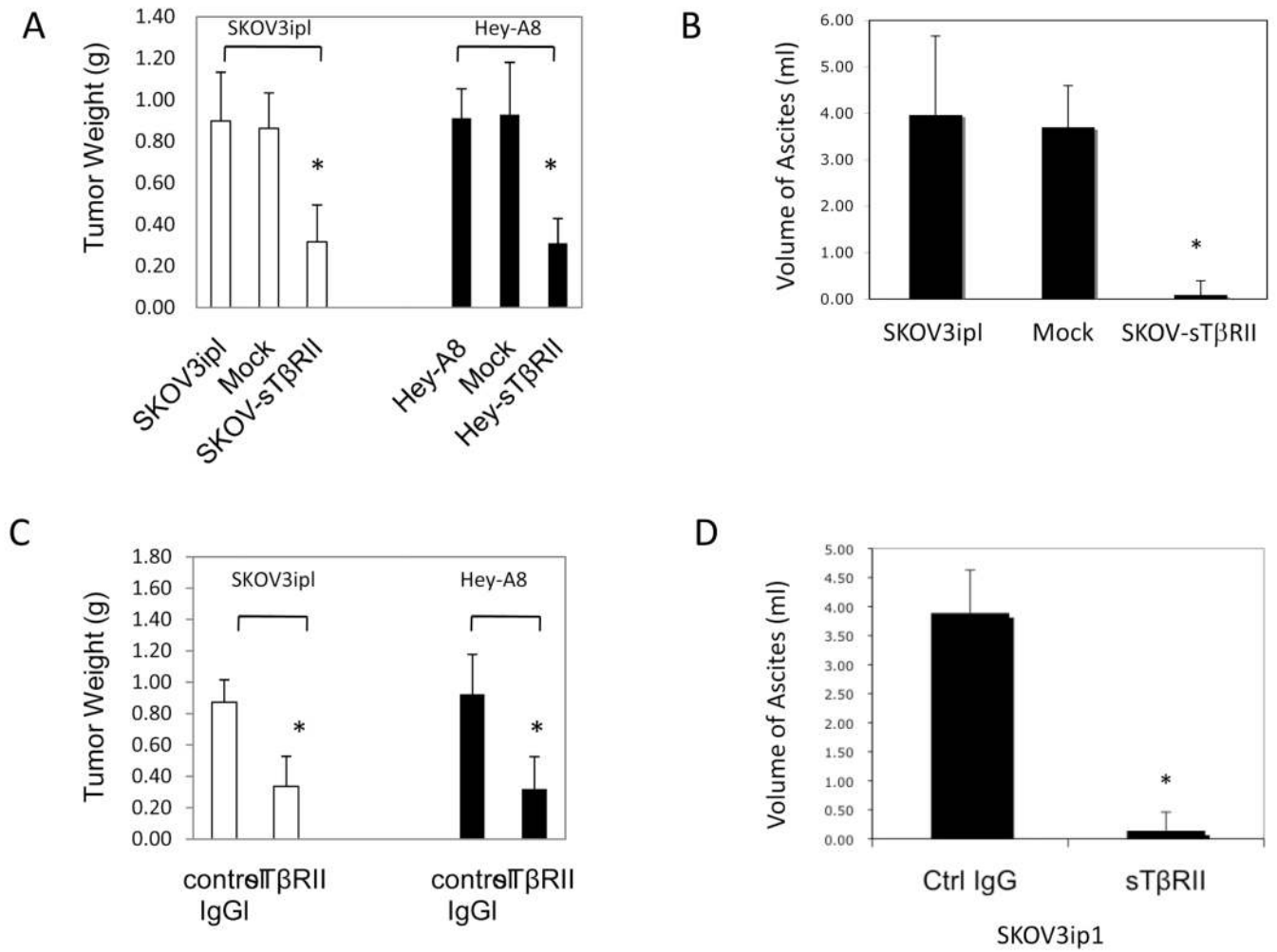
Figure 2.
(A) Transfection of sTβRII decreased SKOV3ip1 and Hey-A8 tumor weight, and (B) volume of ascites in SKOV3ip1 tumor bearing mice. (C) Recombinant sTβRII treatment decreased SKOV3ip1 and Hey-A8 tumor weight, and (D) volume of ascites in SKOV3ip1 tumor bearing mice. n=10.
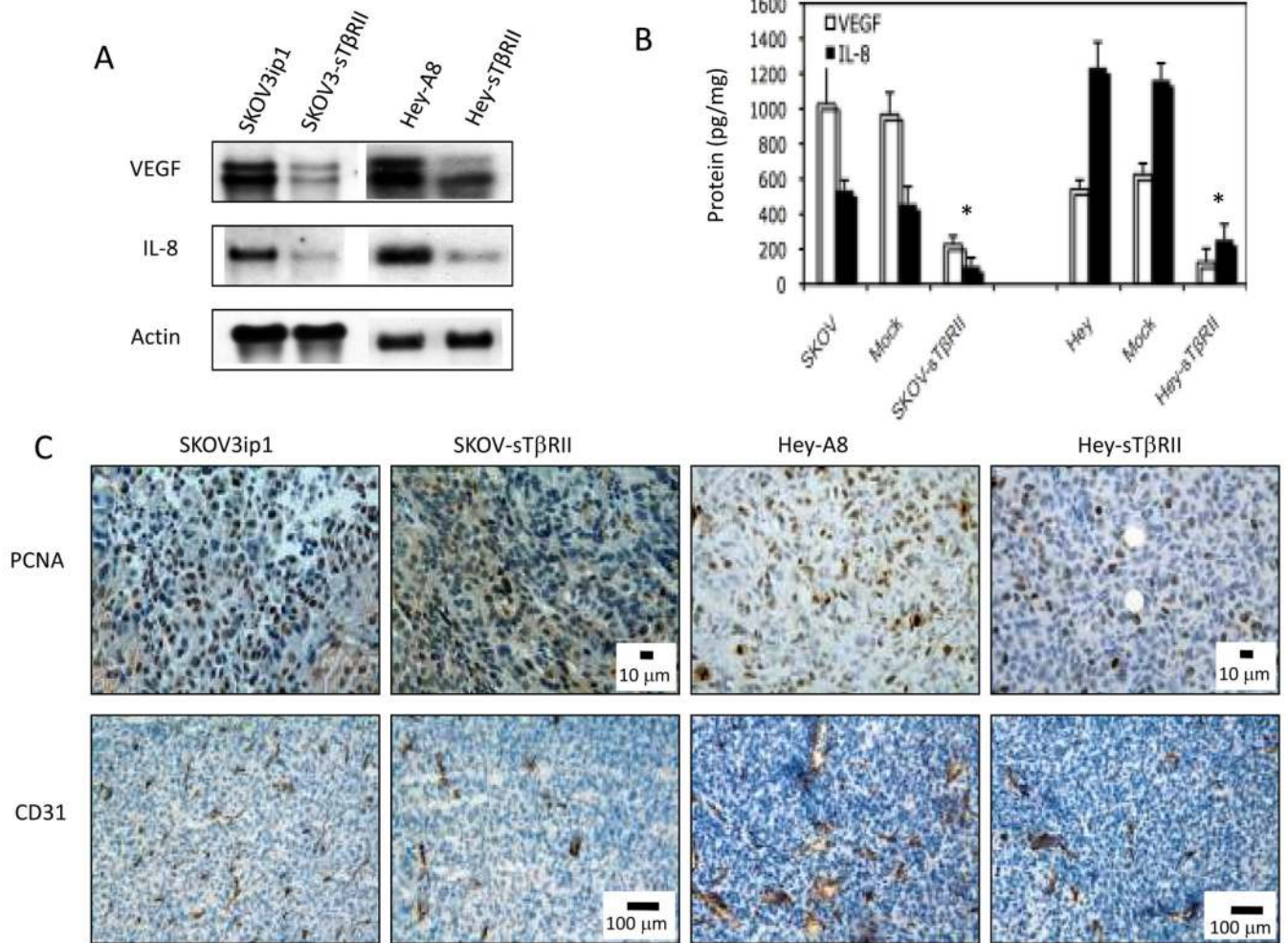
Figure 3.
Blocking TGF-β signaling decreased VEGF and IL-8 expressions. Parental, and sTβRII transfected SKOV3ip1 and Hey-A8 cells were cultured under confluent conditions. (A) mRNA was extracted and Northern blot analysis was performed. Representative of three independent experiments is shown. (B) Protein extracts from parental, mock- and sTβRII-transfected tumor tissues were analyzed by human VEGF and IL-8 ELISA. (C) Frozen sections of tumors obtained from parental and sTβRII transfected SKOV3ip1 and Hey-A8 tumors were analyzed for PCNA and CD31 levels by immunohistochemistry staining.
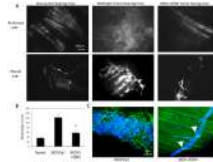
Figure 4.
(A) Fluorescent microscopy of diaphragm lymphatic vessels highlighted by injection of FITC-dextran. (B) Lymphatic vessel diameter in the pleural side of the diaphragm was quantified using a macro in ImageJ. (C) Lymphatic vessels valves were visualized by anti-CD31 (green) and anti-LYVE-1 (blue) double staining; arrows point to valves.
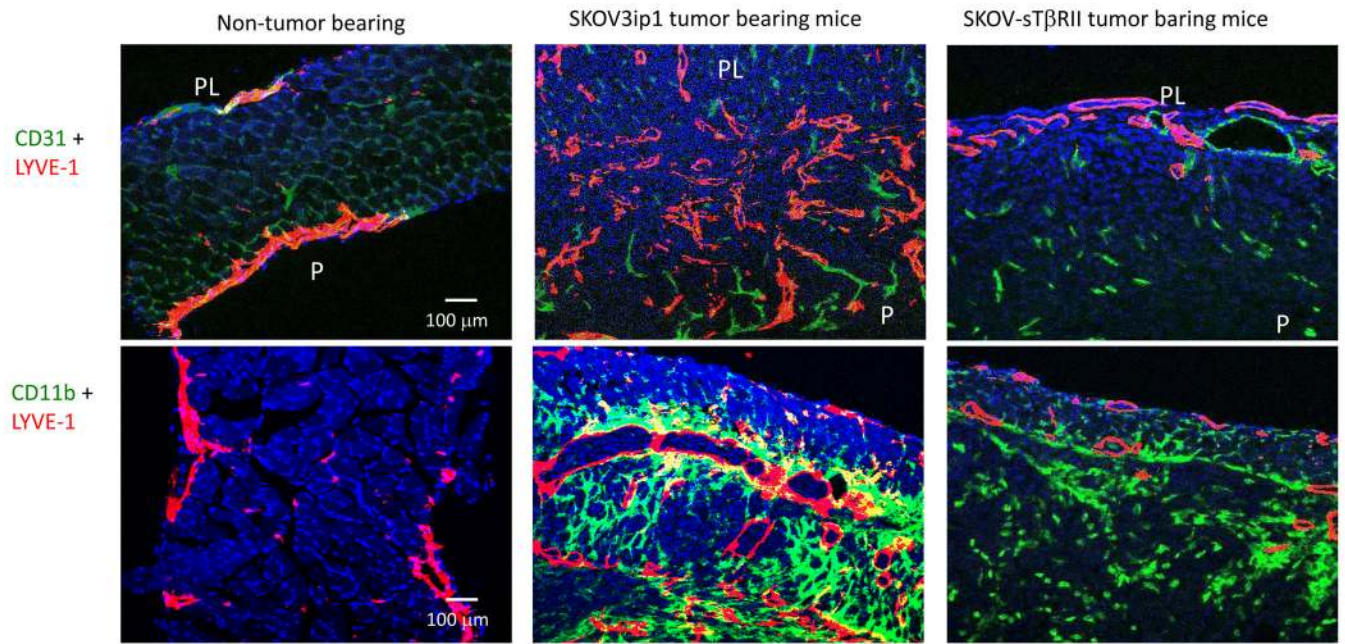
Figure 5.
Blocking tumor and host TGF-β signaling decreased diaphragm lymphangiogenesis. We performed LYVE-1/CD31 and LYVE-1/CD11b double staining in cross-section of the diaphragms from non-tumor-bearing mice, SKOV3ip1 and SKOV-sTβRII tumor-bearing mice. Diaphragm from mice bearing size-matched parental SKOV3ipl and SKOV-sTβRII tumors were used. PL, pleural side; P, peritoneal side. In LYVE-1/CD31 double staining: red, LYVE-1 staining; green, CD31 staining; blue, DAPI. In LYVE-1/CD11b double staining: red, LYVE-1 staining; green, CD11b staining; blue, DAPI.
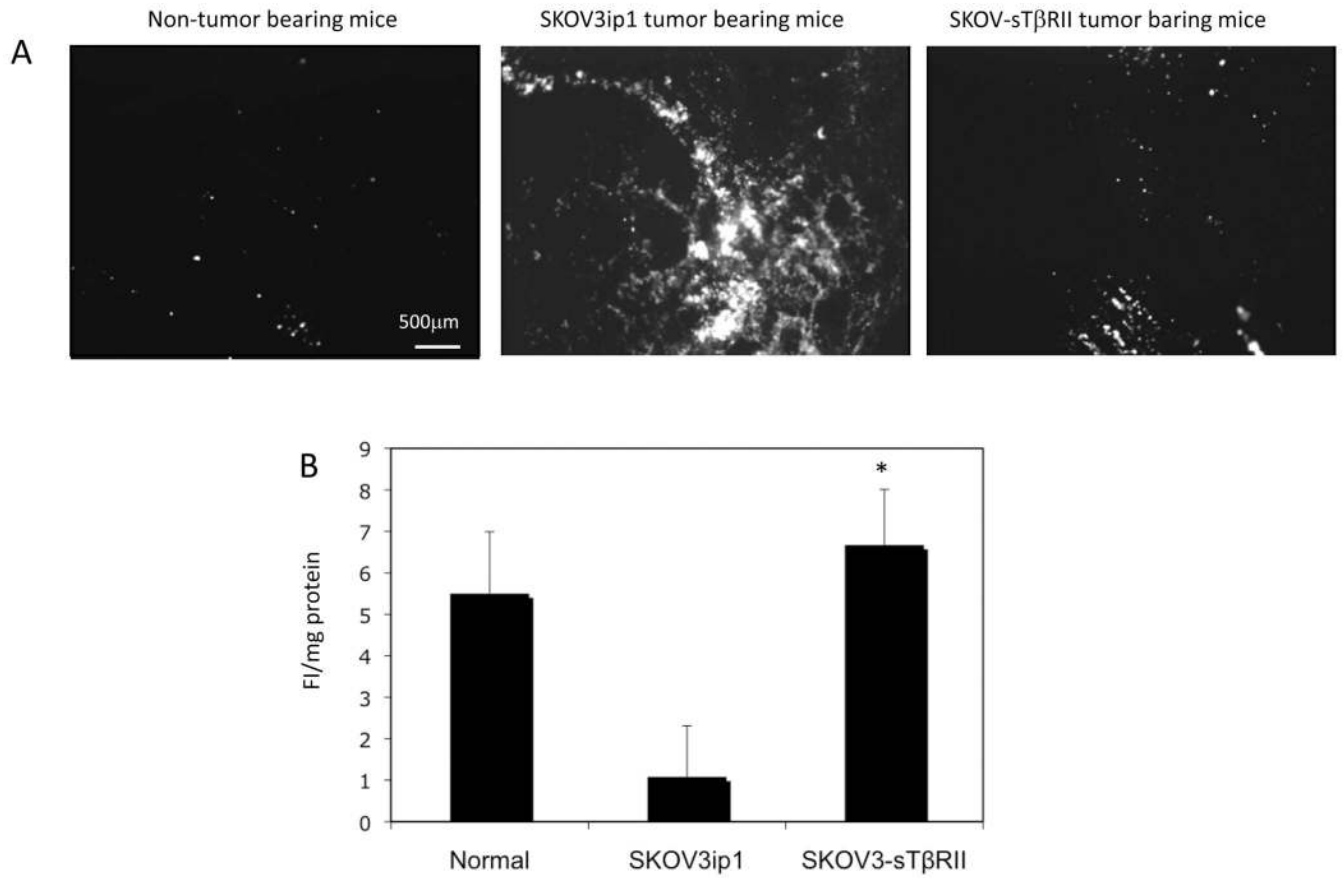
Figure 6.
(A) Fluorescent microscopy of the fluorescent beads in diaphragm. (B) CMLNs were collected and homogenized. Fluorescent intensity of the lysates was determined using a fluorescent microplate reader.